p-ISSN: 2301-6663, e-ISSN: 2477-250X
URL: http://ojs.ummetro.ac.id/index.php/turbo

The effect of curvature ratio towards the fluid flow characteristics in bend pipe based on numerical methods

James Julian[1*], Fitri Wahyuni[2], Waridho Iskandar[3], Rifqi Ramadhani[4]

[1-4]Teknik Mesin, Fakultas Teknik, Universitas Pembangunan Nasional Veteran Jakarta
Jalan RS. Fatmawati Raya, Pd. Labu, Kec. Cilandak, Kota Depok, Jawa Barat, Indonesia
**Corresponding author*: zames@upnvj.ac.id

Abstract

Internal flows in pipes are studied in greater depth and comprehensiveness in research. The computation done by using RANS equation. In particular, this study uses two equations turbulence model which is k-ε turbulence model. Mesh with 2×10^6 element is used because it is a mesh with lowest error. The research focuses on the effect of the curvature ratio (Rc) at the bend on changes in fluid flow characteristics. The Rc variations chosen in this study were 0.01, 0.02, and 0.03. The pipe diameter is 0.01 m, resulting in Rc/D=1, Rc/D=2, and Rc/D=3. At Rc/D=1, the maximum fluid flow velocity is in an area closer to the inner core than the outer core. The fluid velocity distribution is also more even if Rc/D=1 is enlarged. The fluid flow separation appears in the pipe with Rc/D=1, but the fluid flow separation in Rc/D=2 and Rc/D=3 is not visible. The separation is at α=75.96º, while the reattachment location is at x/D=0.014.
Keywords: computation; curvature ratio; diameter; internal flows; pipe bend.

Introduction

Fluid is a substance that can easily be continuously deformed when shear stress is applied [1,2]. From the point of view of its location, fluid flow is divided into two types, i.e., internal and external flow [2,3]. External flow is a fluid flow that flows without being restricted by a solid surface [4]. External fluid flows can be found in fluid flows around vehicles and flow around wind turbines [1,5]. Meanwhile, internal flow is defined as a flow limited by the presence of a wall or a solid object [6,7]. The internal fluid flow is also close to human life [8,9]. Internal flow is generally found in internal combustion engines and flows in pipes. The shape of the pipe greatly influences the flow of the pipe. A straight pipe's flow differs from the fluid flow of a bend pipe. A pipe bend of 90º is an essential part of a piping system. A pipe bend of 90º can provide flexibility in fluid distribution. Various aspects characterize flow in a bend pipe: separation, secondary flow, and unsteadiness. All of these aspects are generally influenced by the Reynolds number and the bends' curvature radius.

The study of flow in pipes has been carried out in the last few decades. Analysis has been carried out using various methods such as experimental, theoretical, and numerical. Weske (1948) carried out an experimental study to investigate the velocity distribution at the outlet of a pipe bend. The study was carried out with various cross-sectional shapes of pipes, such as circles, ellipses, squares, and rectangles. The analysis was carried out on the Reynolds number with a range of 0.2 to 0.6 × 106 [10]. Sudo et al. (1998) conducted experiments on a turbulent flow 90º pipe with Rc/D=2. The study used a hot wire to measure streamwise and circumferential velocity. The Reynolds number used is 60,000 [11]. Dutta et al. studied a 90º pipe bend using a variety of high Reynolds numbers. The method used is computational by using the k-epsilon turbulence model equation. The result is that increasing the Reynolds number can create a velocity profile on the inner core pipe to

DOI: http://dx.doi.org/10.24127/trb.v12i1.2564
Received 3 April 2023; Received in revised form 20 May 2023; Accepted 21 May 2023
Available online 1 Juni 2023

recover fully developed flow by slowing down the speed and accelerating the fluid flow velocity around the outer core. The Reynolds number value also affects fluid flow separation in the pipe. As the Reynolds number increases, the fluid flow separation will move upstream. Meanwhile, increasing the Reynolds number makes the reattachment move closer downstream. Areas of low velocity are found near the inner core of the bend. This low-speed area is the forerunner of flow separation [12]. Kim (2014) characterizes the secondary flow of a 90º elbow in a turbulent pipe flow. The study was carried out experimentally and computationally. This study concludes that there is a similarity between the fluid flow velocity profiles in the Reynolds number range of 50,000 to 200,000. The swirly intensity at the mean tangential velocity decreases exponentially along the flow after the elbow. In addition, it can be seen that the weekly characteristics depend on the Reynolds number [13].

Overall, if accumulated, many of the studies mentioned above have conducted various studies of a 90º pipe bend. Variations common in the various studies above are variations in the Reynolds number. As previously mentioned, the Reynolds number greatly influences the characterization of the fluid flow in the bend. However, one other effect that has not been studied is related to the radius curvature. Therefore, this study aims to observe and study the effect of the curvature radius on the fluid flow characteristics in a 90º pipe bend. Various fluid flow characteristics studied are velocity profile, streamlined fluid flow, separation point, and reattachment. Thus, this research will obtain additional data related to the 90º pipe bend.

Methods

1. Problem definition

This study was done by modeling fluid flow in a bend pipe with a curvature angle of 90º. The pipe diameter uses a constant value of 0.01m. However, this study varied the curvature ratio (Rc) with sizes of 0.01 m, 0.02 m, and 0.03 m. Thus, this study varies the three Rc/D, namely 1, 2, and 3. The fluid used in the pipe is water to be analyzed in this study. The Reynolds number is kept constant at 6×10^4. The overall dimensions of the simulation model can be seen in Figure 1 [14].

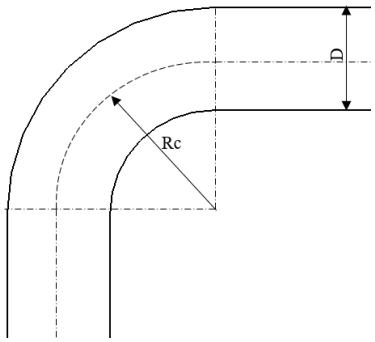

Figure. 1 Geometry

2. Problem definition

The type of mesh in this study is a three-dimensional structured mesh with hexahedral elements. The advantage of this type of mesh is that it can simplify computation and has a low cost per iteration. This study prepared three types of mesh, each differentiated based on the number of elements. The number of meshes prepared is 2×10^6, 10^6, and 5×10^5. To determine the mesh used for further research is the analysis of the mesh independence test. The mesh that used in this study is depicted in Figure 2.

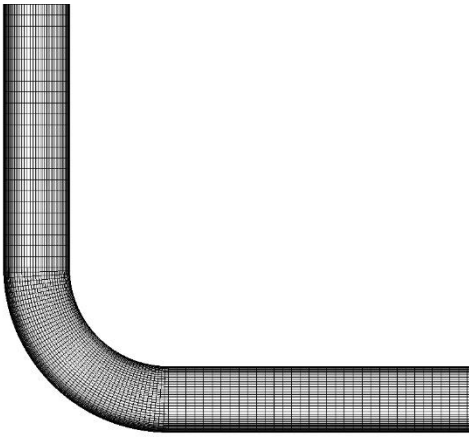

(a) Pipe length

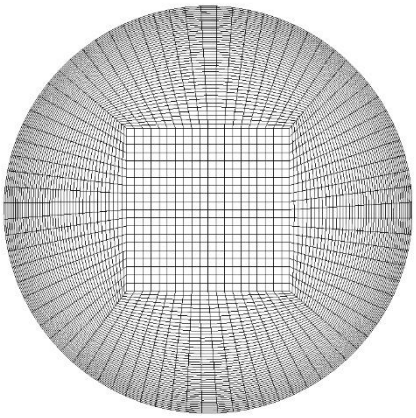

(b) Detail of bend

Figure 2. Three-dimensional structured mesh

3. Governing equation

The Reynolds Averaged Navier-Stokes (RANS) equation is used to solve cases of fluid flow in bend pipes. This study uses the second order to analyze the steady flow. Pressure velocity coupling is set with the Coupled algorithm [15]. All fluid properties in this study use constant properties [16]. The RANS equation in this study models fluid flow as an incompressible flow [1]. In general, the RANS equation for incompressible flow consists of two equations: the equation for the conservation of mass and the equation for the conservation of momentum. The equation for the conservation of mass can be seen in equation 1. The equation for the conservation of momentum can be seen in equation 2.

$$\frac{\partial u_i}{\partial x_i} = 0 \tag{1}$$

$$\frac{\partial u_i}{\partial t} + u_j \frac{\partial u_i}{\partial x_j} = f_i - \frac{1}{\rho}\frac{\partial p}{\partial x_i} + \upsilon \frac{\partial^2 u_i}{\partial x_i \partial x_j} \tag{2}$$

4. Turbulence model

Because the flow in the pipe is analyzed at the Reynolds number 6×10^4, it can be ascertained that the fluid flow in the pipe is turbulent. Therefore, this study uses a turbulence model to accompany the RANS equation. There are many turbulence models available in the RANS equation. The selection of the turbulence model requires various considerations, such as the capabilities and also limitations of the turbulence model. In particular, this study uses the standard *k-ε* turbulence model. The *k-ε* turbulence model performs well when modeling flow in either one or two phases. The mathematical equation of this turbulence model can be seen in equations 3 and 4.

$$\frac{\partial (pk)}{\partial t} + \frac{\partial (pku_i)}{\partial x_i} = \frac{\partial}{\partial x_j}\left[\frac{\mu_t}{\sigma_k}\frac{\partial k}{\partial x_j}\right]_i + 2\mu_t E_{ij} E_{ij} - \rho\varepsilon \tag{3}$$

$$\frac{\partial (p\varepsilon)}{\partial t} + \frac{\partial (p\varepsilon u_i)}{\partial x_i} = \frac{\partial}{\partial x_j}\left[\frac{\mu_t}{\sigma_\varepsilon}\frac{\partial k}{\partial x_j}\right]_i + C_{1\varepsilon}\frac{\varepsilon}{k} 2\mu_t E_{ij} E_{ij} - C_{2\varepsilon}\rho\frac{\varepsilon^2}{k} \tag{4}$$

Results and Discussion

1. Mesh independence test

To ensure the computation results is verified, this study use mesh independece test. The method that used is Richardson Extrapolation. This study provides theree mesh variations for verified. Every mesh is distinguished by the elements number i.e., 5×10^5, 1×10^6 and 2×10^6. Each stage of the mesh independence test was carried out as in the study of Julian et at [17]. The properties used in the mesh independence test are the velocity variables at positions x=0.02, y=0, and z=0 (the center point of the outlet bend). All variables are then given in table 1. The mesh variations are in the convergence index range where the results of the mesh independence test show that $\frac{GCI_{coarse}}{GCI_{fine}(r^p)} \approx 1$[18]. The mesh independence test results show that the mesh closest to the parameter results is a fine mesh with a velocity value of 7.423, where the parameter value is 7.425. In other words, the mesh with the lowest error is fine. Therefore, other computational processes will use a fine mesh. The results of the mesh independence test are depicted in Figure 3.

Tabel 1. Mesh independece test

Mesh categories	Number of elements	Velocity	Diskrit code
Fine	2×10^6	7.423	f_1
Medium	1×10^6	7.418	f_2
Coarse	5×10^5	7.395	f_3

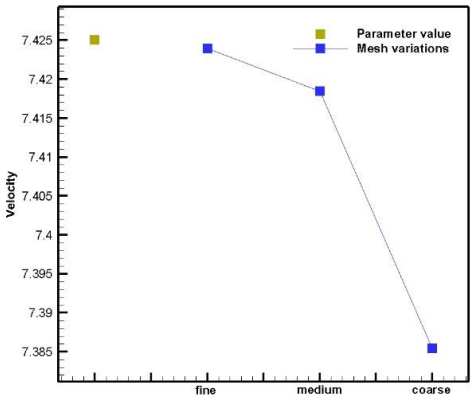

Figure 3. Mesh independece test results

2. Validation

The data obtained from this study were then validated by comparing it with research with the results obtained from other studies. The comparative data used were obtained through a study by Dutta et al. The results of the validation of the data can be seen more specifically in Figure 4. The data was taken at the outlet location of the pipe bend with Rc/D=2, as shown in Figure 3 (b). Based on the validation results, it can be seen that the data in this study showed identical results to data from Dutta et al., especially at r/R=-0.15 to 0.5. At r/R=-0.5 to -0.15, the data shows a slight difference, but the trend shown is still the same. The negative sign indicates the location is closer to the inner core. Thus, the data from this study are quite valid.

3. Research results

With the same tapping location as in the validation, an analysis of changes in Rc was carried out on the velocity profile of the bend outlet. The center of the pipe cross-section is located at r/R=0. It can be seen that when r/R= 0.2 to 0.5, the pipe with Rc/D=3 shows the highest speed when compared to

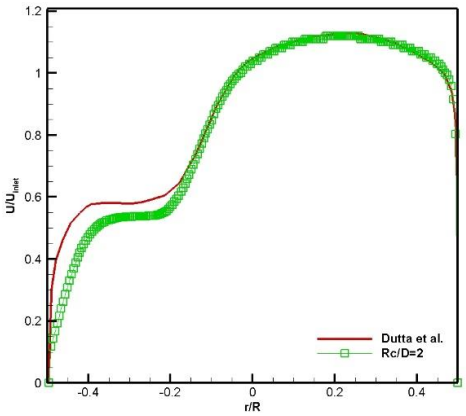

(a) Velocity profile

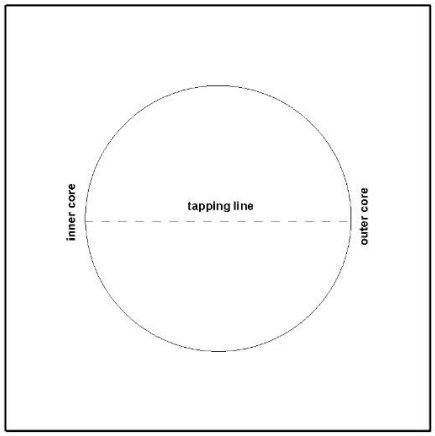

(b) Tapping location

Figure 4. Validation

other variations of Rc/D. However, when the r/R is in the range of -0.1 to 0.2, the pipe with Rc/D=1 has the highest speed. It is caused by the curvature of the pipe, which results in high-speed fluid flow closer to the inner core when it is right in the middle of the bend. Conversely, when Rc/D is enlarged, the high-speed fluid flow is closer to the outer core so that the maximum fluid velocity is in a location that is quite close to the outer core. Meanwhile, when r/R=-0.5 to -0.2, a pipe with Rc/D=3 produces a high velocity. It is due to the pipe's ability to avoid fluid flow separation. However, an anomaly occurs where the velocity at that location is at Rc/D=1 greater than that of the pipe with Rc/D=2. In contrast, the greater the Rc value, the smoother the curvature of a pipe to avoid fluid flow separation [19]. It cannot be explained in Figure 5. Therefore,

it is necessary to analyze the velocity distribution in the outlet bend section.

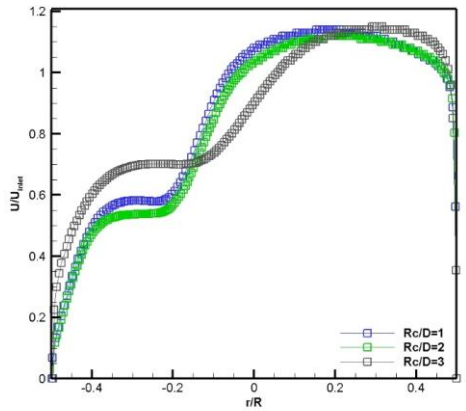

Figure 5. Velocity profile with Rc/D variations

The fluid flow velocity contour can show the velocity distribution along the pipe cross-section at the outlet bend. The fluid flow velocity contour can be seen in Figure 6. An apparent increase in the Rc/D value can make the distribution of fluid velocity more even. Separation of fluid flow at the outlet bend is seen when Rc/D=1. Meanwhile, when Rc/D=2 and Rc/D=3, the fluid flow separation is not visible. However, in pipes with Rc/D=2, there is a fairly low-velocity fluid flow. This fluid flow is at the tapping location of the velocity profile and is very thin when viewed from the outlet bend cross-section, which causes the velocity profile Rc/D=1 to be greater than Rc/D=1.

Figure 6 shows a longitudinal cross-section of each pipe in the bend section. It can be seen more clearly that there is a separation of fluid flow at the location of the inner core at Rc/D=1. At first glance, the shape of the fluid flow separation is shown in study 6 [20]. Pipes with sizes Rc/D=2 and Rc/D=3 do not show any fluid flow separation. It is just that there is an area with low-speed fluid flow. This low-velocity fluid area is the forerunner of the formation of secondary flow in the pipe. The area of this low-speed area will get smaller as Rc/D increases. In Figure 7, it can also be seen that there is an increase in speed in the inner core when Rc/D is reduced.

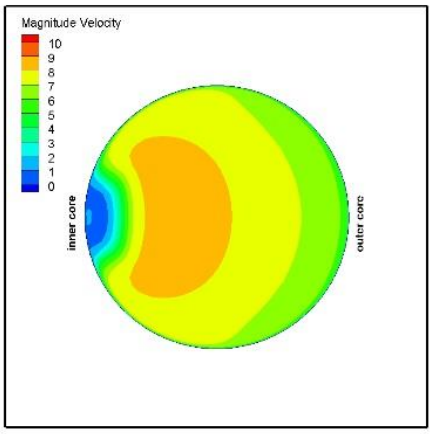

(a) Rc/D=1

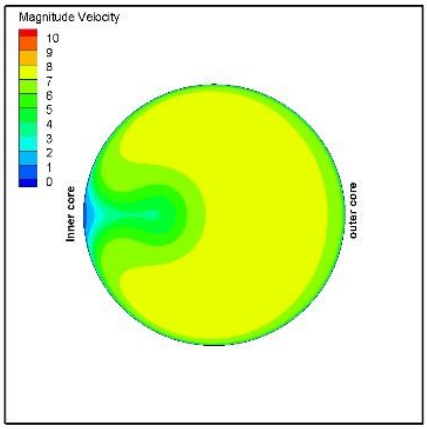

(b) Rc/D=2

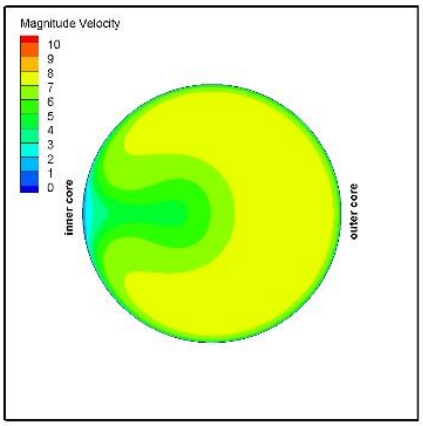

(c) Rc/D=3

Figure 6. Velocity contour on outlet bend

In particular, this paragraph discusses the separation of fluid flows. The separation of fluid flow is initialized by a point which called separation point. Further, a point which the separation of fluid flow end is called reattachment point [19]. The location of separation point in this study is

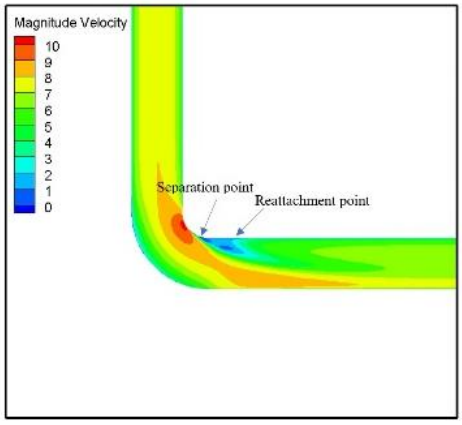

(a) Rc/D=1

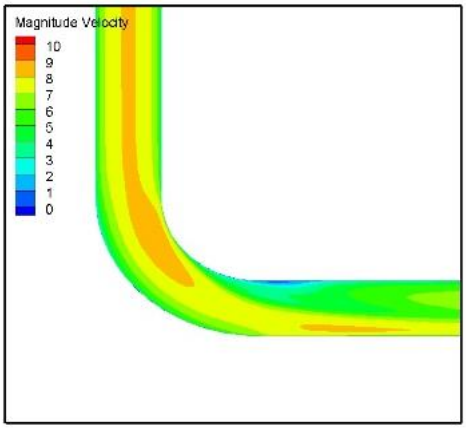

(b) Rc/D=2

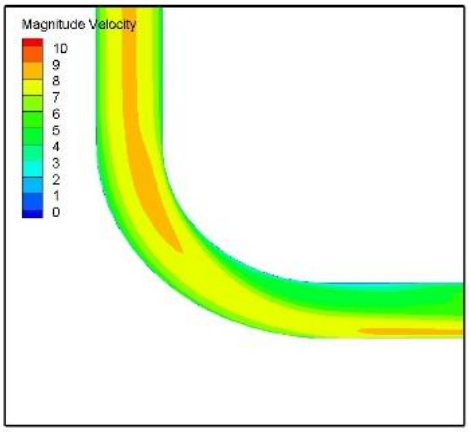

(c) Rc/D=3

Figure 7. Velocity contour on pipe bend

in α=75.96º. The location of the separation point is expressed in terms of the ratio between the outlet bend distance and the pipe diameter. The reattachment point measured in this study was at x/D=0.014. The method of searching and measuring the separation and reattachment points is carried out according to [20]. Overall, the speed profile at the separation point (SP), middle point (MP), and reattachment point (RP) can be seen in Figure 8.

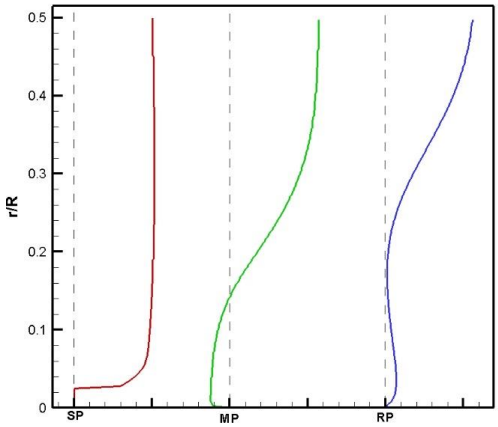

Figure 8. Velocity profile on separation point, separation, reattachment

2. Kesimpulan

This study discusses more deeply the flow in a 90º bend pipe. Furthermore, this research studies the effect of changes in Rc on the characteristics of the fluid flow through the bend. When Rc/D=1, the maximum velocity of the fluid is precisely r/R=-0.1 to r/R=0.2. It is caused by the extreme curvature of the pipe so that the high-velocity fluid is closer to the inner core. The high-speed fluid flow is closer to the outer core when the Rc/D value is enlarged to 2 and 3. The greater the Rc/D value, the more even the velocity distribution at the outlet bend will be. The fluid flow separation can be seen at the bend pipe outlet with Rc/D=1. Meanwhile, at Rc/D=2 or Rc/D=3, there is no fluid flow separation. The location of the fluid flow separation is at α=75.96º, while the location of the

Referensi

[1] W. Harinaldi, S. Adhika, and J. Julian, “The comparison of an analytical, experimental, and simulation approach for the average induced velocity of a dielectric barrier discharge (DBD),” in The 10th

International Meeting of Advances in Thermofluids (IMAT 2018): Smart City: Advances in Thermofluid Technology in Tropical Urban Development, 2019, p. 020027.

[2] J. Julian, R. Difitro, and P. Stefan, "The effect of plasma actuator placement on drag coefficient reduction of Ahmed body as an aerodynamic model," International Journal of Technology, vol. 7, no. 2, pp. 306–313, 2016.

[3] J. Julian, Harinaldi, Budiarso, C.-C. Wang, and M.-J. Chern, "Effect of plasma actuator in boundary layer on flat plate model with turbulent promoter," Proc Inst Mech Eng G J Aerosp Eng, vol. 232, no. 16, pp. 3001–3010, 2018.

[4] E. A. Kosasih, R. F. Karim, and J. Julian, "Drag reduction by combination of flow control using inlet disturbance body and plasma actuator on cylinder model," Journal of Mechanical Engineering and Sciences, vol. 13, no. 1, pp. 4503–4511, 2019.

[5] J. Julian and R. F. Karim, "Flow control on a squareback model," International Review of Aerospace Engineering, vol. 10, no. 4, pp. 230–239, 2017.

[6] R. F. Karim and J. Julian, "Drag reduction due to recirculating bubble control using plasma actuator on a squareback model," in MATEC Web of Conferences, EDP Sciences, 2018, p. 01108.

[7] J. Julian, "The effect of plasma actuator utilization to the reduction of aerodynamic drag of cylinder and box models," 2016.

[8] Harinaldi, M. D. Kesuma, R. Irwansyah, J. Julian, and A. Satyadharma, "Flow control with multi-DBD plasma actuator on a delta wing," Evergreen, vol. 7, no. 4, pp. 602–608, 2020, doi: 10.5109/4150513.

[9] H. Harinaldi, B. Budiarso, J. Julian, and A. WS, "Drag Reduction in Flow Separation Using Plasma Actuator in a Cylinder Model," 2015.

[10] J. R. Weske, Experimental investigation of velocity distributions downstream of single duct bends, no. 1471. National Advisory Committee for Aeronautics, 1948.

[11] K. Sudo, M. Sumida, and Hje. Hibara, "Experimental investigation on turbulent flow in a circular-sectioned 90-degree bend," Exp Fluids, vol. 25, no. 1, pp. 42–49, 1998.

[12] P. Dutta, S. K. Saha, N. Nandi, and N. Pal, "Numerical study on flow separation in 90° pipe bend under high Reynolds number by k-ε modelling," Engineering Science and Technology, an International Journal, vol. 19, no. 2, pp. 904–910, 2016.

[13] J. Kim, M. Yadav, and S. Kim, "Characteristics of secondary flow induced by 90-degree elbow in turbulent pipe flow," Engineering Applications of Computational Fluid Mechanics, vol. 8, no. 2, pp. 229–239, 2014.

[14] M. Tanaka, H. Ohshima, and H. Monji, "Numerical investigation of flow structure in pipe elbow with large eddy simulation approach," in ASME Pressure Vessels and Piping Conference, 2009, pp. 449–458.

[15] J. Julian, W. Iskandar, F. Wahyuni, A. Armansyah, and F. Ferdyanto, "Effect of Single Slat and Double Slat on Aerodynamic Performance of NACA 4415," International Journal of Marine Engineering Innovation and Research, vol. 7, no. 2, 2022.

[16] F. C. Megawanto, Harinaldi, Budiarso, and J. Julian, "Numerical analysis of plasma actuator for drag reduction and lift enhancement on

NACA 4415 airfoil," in AIP Conference Proceedings, AIP Publishing LLC, 2018, p. 050001.

[17] J. Julian, W. Iskandar, F. Wahyuni, and dan Nely Toding Bunga, "Jurnal Asiimetrik: Jurnal Ilmiah Rekayasa Dan Inovasi Karakterisasi Efek Co-Flow Jet Sebagai Salah Satu Perangkat kontrol Article information," vol. 4, pp. 185–192, 2022.

[18] W. Iskandar, J. Julian, F. Wahyuni, F. Ferdyanto, H. K. Prabu, and F. Yulia, "Study of Airfoil Characteristics on NACA 4415 with Reynolds Number Variations," International Review on Modelling and Simulations (IREMOS), vol. 15, no. 3, pp. 162–171, Jun. 2022.

[19] J. Julian, W. Iskandar, F. Wahyuni, and F. Ferdyanto, "Computational Fluid Dynamics Analysis Based On The Fluid Flow Separation Point On The Upper Side Of The Naca 0015 Airfoil With The Coefficient Of Friction," Media Mesin: Majalah Teknik Mesin, vol. 23, no. 2, pp. 70–82, 2022.

[20] P. Dutta, S. K. Saha, N. Nandi, and N. Pal, "Numerical study on flow separation in 90° pipe bend under high Reynolds number by k-ε modelling," Engineering Science and Technology, an International Journal, vol. 19, no. 2, pp. 904–910, Jun. 2016, doi: 10.1016/j.jestch.2015.12.005.